

EFFECT OF STRUCTURE AND TEXTURE ON THE MECHANICAL CHARACTERISTICS OF MAGNESIUM ALLOYS PROCESSED BY EQUAL-CHANNEL ANGULAR PRESSING

ВЛИЯНИЕ СТРУКТУРЫ И ТЕКСТУРЫ НА МЕХАНИЧЕСКИЕ ХАРАКТЕРИСТИКИ МАГНИЕВЫХ СПЛАВОВ, ПОЛУЧЕННЫХ РАВНОКАНАЛЬНЫМ УГЛОВЫМ ПРЕССОВАНИЕМ

PhD Martynenko N.S.^{1,2*}, Tokar A.A.^{1,2}, PhD. Serebryany V.N.¹, PhD. Prosvirnin D.V.¹, Prof., Dr. Sci. Terentiev V.F.¹, Prof., Dr. Sci. Raab G.I.³, Prof., Dr. Sci. Dobatkin S.V.^{1,2}, Prof., PhD Estrin Yu.Z.^{4,5}

¹A.A. Baikov Institute of Metallurgy and Materials Science of RAS, Moscow, Russia

²National University of Science and Technology "MISIS", Moscow, Russia

³Ufa State Aviation Technical University, Ufa, Russia

⁴Department of Materials Engineering, Monash University, Clayton, VIC 3800, Australia

⁵Department of Mechanical Engineering, The University of Western Australia, Nedlands, Australia

E-mail: nataliasmartynenko@gmail.com

Abstract: ECAP was carried out with a gradual decrease in temperature and an increase in the number of passes on two medical magnesium alloys: WE43 (Mg-3.56%Y-2.20%Nd-0.47%Zr) and ZX10 (Mg-1.0%Zn-0.3%Ca). It was shown that ECAP leads to a significant refinement of the alloys structure. For ZX10 alloy, the average grain size after ECAP decreased from $\sim 105 \mu\text{m}$ in the initial state to $8 \pm 0.18 \mu\text{m}$ in the longitudinal section and to $4 \pm 0.19 \mu\text{m}$ in the transverse one. For the WE43 alloy, the average grain size was changed from $70 \mu\text{m}$ to $0.69 \pm 0.13 \mu\text{m}$ and the precipitation of particles of the $\text{Mg}_{41}\text{Nd}_5$ phase with an average size of $0.45 \pm 0.18 \mu\text{m}$ was also discovered. At the same time, the grain refinement led to an increase in the strength characteristics of the both alloys (including fatigue strength), and increased prismatic slip activity (along with the formation of an inclined basal texture in ZX10 alloy) led to an increase in their ductility. The alloy structure formed during the ECAP process does not lead to a decreasing in resistance to chemical corrosion.

KEYWORDS: MAGNESIUM ALLOYS, EQUAL CHANNEL ANGULAR PRESSING, ULTRAFINE GRAINED STRUCTURE, TEXTURE, MECHANICAL PROPERTIES, FATIGUE LIFE

1. Introduction

Magnesium alloys have been actively studied in many countries for two decades as medical materials [1-3]. Currently, the most studies are aimed at obtaining the optimal composition and properties of these materials. The development of the compositions of such alloys is complicated by the fact that the selected alloying elements must have good biocompatibility and fulfill their basic properties: strengthen the alloys and increase its corrosion resistance. Therefore, a limited number of elements are now used (Ca [4], Zn [5], Ag [6], Li [7], Sr [8], Mn [9], some rare-earth metals [10-12]), which fall in their characteristics under both criteria. But just only alloying is not enough to obtain optimal properties. Therefore, alloys usually are deformed to improve their mechanical properties. In this sense, severe plastic deformation [13], and in particular equal-channel angular pressing (ECAP) [14], which allows significantly strengthening magnesium alloys by formation an ultrafine grained (UFG) structure, is especially attractive. In addition, the cases of increasing the corrosion resistance of magnesium alloys after formation of UFG structure are known [15, 16]. Therefore, the effect of alloying and ECAP on the structure and properties of two medical magnesium alloys (WE43 and ZX10) was studied in this study.

2. Materials and Methods

Two magnesium alloys were investigated in the work: WE43 (Mg-3.56%Y-2.20%Nd-0.47%Zr) and ZX10 (Mg-1.0%Zn-0.3%Ca). In the initial state, the WE43 alloy was homogenized at 525°C for 8 hours and then air cooled. The ZX10 alloy was also subjected to homogenization at 450°C for 3 hours and then water quenched. The Bc ECAP route was carried out on the machine with a channel intersection angle of 120° with a gradual decrease in the deformation temperature and an increase in the number of passes. For WE43 alloy, the ECAP temperature decreased from 425 to 300°C with a step of 25°C and 2 passes at each temperature ($N_\Sigma = 12$). For the ZX10 alloy, stepwise ECAP was performed with a decrease in temperature from 400 to 300°C with a step of 25°C and also 2 passes at each temperature ($N_\Sigma = 10$) (Figure 1).

The microstructure was examined using an Axio Observer D1m Carl Zeiss optical microscope and an electron microscope JEM-1400 (Jeol, Japan) operating at a voltage of 120 kV. Foils for TEM analysis after ECAP were cut in the longitudinal direction,

mechanically ground up to $180 \mu\text{m}$ and then subjected to ion-bombardment on a GATAN 600 unit. The size of the microstructural units was estimated by the method of random sections using the Image ExpertPro 3 software.

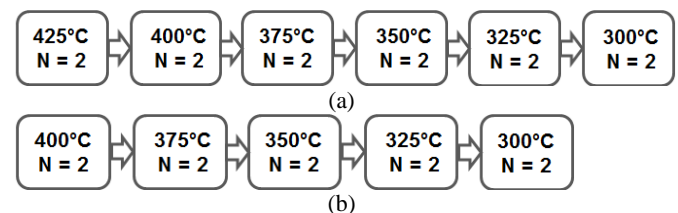


Figure 1 - The ECAP processing regimes employed (N denotes the number of passes at a given temperature)

Texture analysis was carried out using X-ray diffraction in a Rigaku Ultima IV diffractometer with the $\text{CuK}\alpha$ radiation in the reflection mode. Five complete pole figures $\{00.4\}$, $\{20.2\}$, $\{10.2\}$, $\{10.3\}$, $\{11.0\}$ were obtained with a maximum inclination angle $\alpha_{\text{max}} = 70^\circ$ and a step of 5° in the radial angle α and the azimuth angle β on a pole figure. The orientation distribution functions (ODFs) were calculated from the measured pole figures presented as a superposition of a large number (1000) of standard distributions with a small scatter. The centers of standard functions were located on a regular three-dimensional grid in the orientation space [17]. With these ODFs, complete pole figures were also calculated. The volume fractions of the major orientations were estimated using the ODFs as described in [17]. Using the Euler angles and the volume fractions of the orientations, the generalized Schmid factors for the existing deformation systems and the inverse orientation factors were calculated, as described in [18].

The mechanical properties were evaluated through uniaxial tensile tests carried out at room temperature in an Instron 3382 testing machine with an extension rate of 1 mm/min on 33 mm long dog bone-shaped specimens with a gauge length of 15.0 mm and diameter of 3.0 mm. The fatigue tests were carried out under cyclic tension using an ElectroPulsTME3000 machine (testing frequency of 30 Hz, stress ratio $R = 0.1$).

The corrosion properties were investigated by the weight loss method upon immersion of specimens in a 0.9% NaCl solution at

37°C for 4 weeks. Before weighing the specimens after immersion, the corrosion products were removed according to ASTM_G1-03-E.

3. Results and Discussion

The study of the alloys microstructure in the initial state showed that after homogenization in both cases a uniform structure with equiaxed grains is formed (Figure 2 a, b) (an average grain size of $\sim 70 \mu\text{m}$ for the WE43 alloy and $\sim 105 \mu\text{m}$ for the ZX10 alloy). The formation of smaller grains in the case of the WE43 alloy, even despite the longer homogenization duration, is probably associated with the presence of Zr in its composition, which use as a modifier for refinement the structure. In addition, due to the low diffusion rate of rare-earth metal atoms in the case of WE43 alloy, more thermal energy is required to dissolve the phase. ECAP leads to a significant refinement of the structure of both alloys. An ultrafine grained structure with an average grain size of $0.69 \pm 0.13 \mu\text{m}$, as well as globular particles of the $\text{Mg}_{41}\text{Nd}_5$ phase [19] with an average size of $0.45 \pm 0.18 \mu\text{m}$ are formed after ECAP in the WE43 alloy (Figure 2 c). At the same time, ECAP in the ZX10 alloy leads to the formation of a rather inhomogeneous structure elongated along the pressing direction with an average grain size of $8 \pm 0.18 \mu\text{m}$ in the longitudinal section (Figure 2 d) and $4 \pm 0.19 \mu\text{m}$ in the transverse one. The formation of larger grains, in comparison with the previous alloy, is probably associated with a smaller number of ECAP passes, as well as a lower temperature recrystallization of the alloy. The second phase particles were not found in this alloy after ECAP.

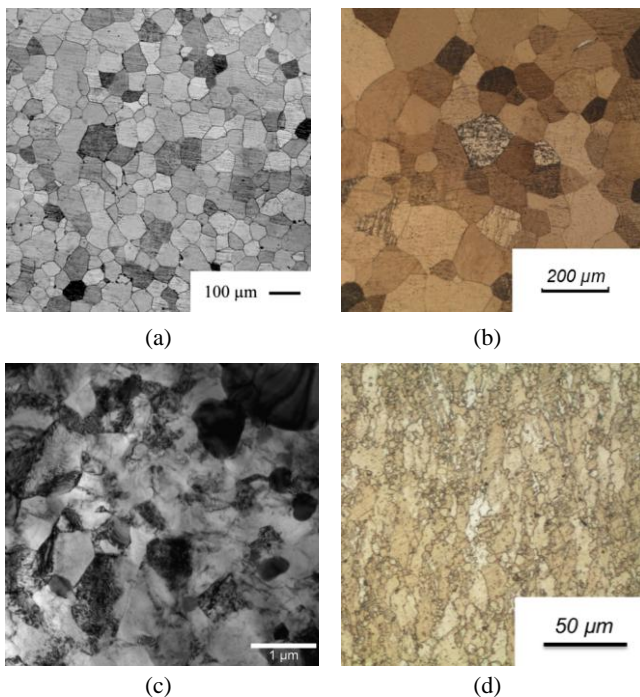


Figure 2 – The microstructure of the WE43 alloy (a, c) and the ZX10 alloy (b, d) in homogenized (a, b) and deformed (c, d) states

The study of the mechanical properties of the alloys showed that the formation of a more dispersed structure after ECAP in the case of the WE43 alloy most significantly strengthened the alloy. So in the initial state, a yield stress (YS) of the WE43 alloy was 161 MPa, an ultimate tensile strength (UTS) - 234 MPa, and an elongation (EI) - 9%. But these characteristics increased to 260 MPa, 300 MPa, and 12.4% after ECAP, respectively. The yield stress was 92 MPa, the ultimate tensile strength - 194 MPa, and the elongation - 12.8% in the case of the initial state of the ZX10 alloy. After ECAP, the ductility is almost doubled to 23.9%, while the strength remains almost unchanged (the yield stress is 106 MPa and the ultimate tensile strength is 215 MPa) (Table 1).

Table 1 – Mechanical properties of WE43 and ZX10 alloys in the initial state and after ECAP processing

	Conditions	UTS, MPa	YS, MPa	EI, %
ZX10	Initial state	194	92	12.8
	ECAP	215	106	23.9
WE43	Initial state	234	161	9.0
	ECAP	300	260	12.4

As noted earlier, the increase in strength characteristics is associated with the grain refinement. However, for example, for ZX10 alloy, grain refinement after ECAP more than 10 times does not lead to a significant increase in strength. In addition, for both alloys, despite the refinement of the structure, an increase in ductility is observed. That is, it can be assumed that there are additional factors affecting the final properties. In magnesium alloys, in addition to structure, the transformation of texture also contributes to the change in mechanical properties. Therefore, to assess the contribution of the texture to the change in the mechanical properties of materials, direct pole figures of the alloys were constructed before and after ECAP, and the orientation factors of the main deformation systems and twinning were calculated (Figure 3 and Table 2).

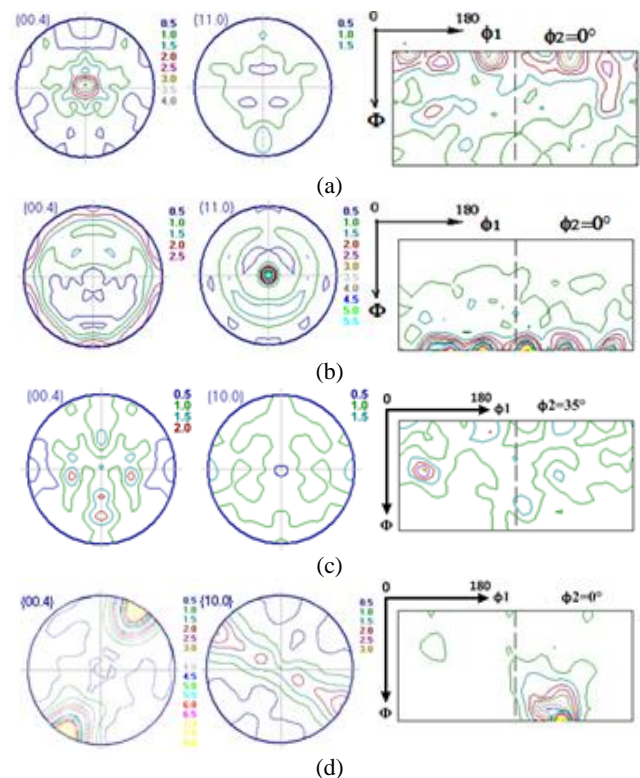


Figure 3 - (00.4) and (11.0) pole figures and ODF sections at $\phi_2 = \text{const}$ for the WE43 (a, b) and ZX10 (c, d) alloys in the initial states (a, c) and after ECAP processing (b, d)

The texture analysis showed that a cardinal change of texture type occurs from a sharp basal texture in the initial state to a sharp prismatic texture in the case of ECAP of the WE43 alloy (Figure 3 a, b). It is known that activation of prismatic slip in magnesium alloys leads to an improvement in their ductility, which we observe for the WE43 alloy. At the same time, the magnesium alloys after ECAP are also characterized by the formation of an inclined basal texture, which has a beneficial effect on the ductility, but does not improve (and often worsens) their strength [19, 20]. We observe a similar situation in the case of the ZX10 alloy, where ECAP leads to the transformation of a diffused basal texture into a sharp basal texture inclined by 80-85° (Figure 3 c, d). At the same time, in the case of alloys with rare-earth metals, fine particles are deposited in the basal planes, which make it difficult to slip dislocations along

them [21]. This leads to partial inhibition of the basal slip and activation of the prismatic one, which does not lead to deterioration in ductility and strength. We observe a similar situation for the WE43 alloy. Moreover, a decrease in the values of orientation factors for prismatic slip planes also indicates an increased likelihood of prismatic slip in the alloys after ECAP (Table 2). The probability of basal and pyramidal slip activity, as well as twinning in the case of WE43 alloy, is reduced. Twinning activity in the case of the ZX10 alloy remains unchanged.

Table 2. Orientation factors for WE43 and ZX10 alloys in the initial state and after ECAP processing

Conditions	Basal {0001} <1120>	Prismatic {1010} <1120>	Pyramidal <c+a>	Twinning {1012} <1011>
Initial state (WE43)	4.6	6.2	4.1	4.0
ECAP (WE43)	6.0	4.3	5.0	5.0
Initial state (ZX10)	4.4	5.1	4.7	4.8
ECAP (ZX10)	5.9	3.9	4.9	4.8

The Figure 4 shows the results of the fatigue life study of the both studied alloys before and after ECAP.

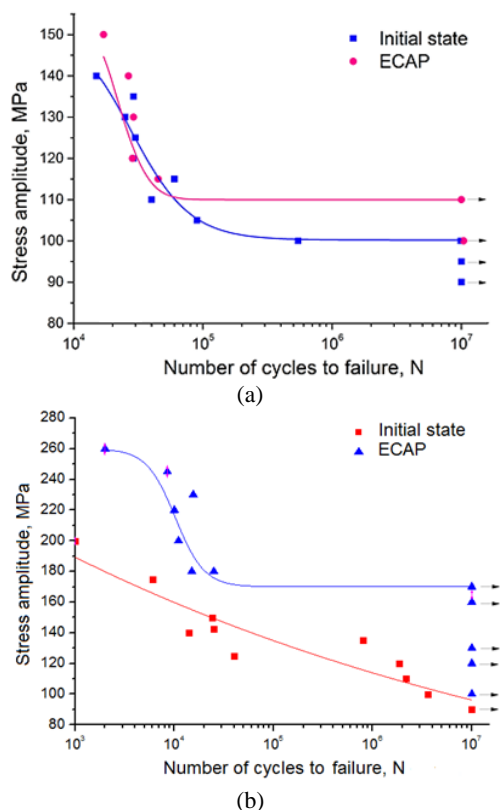
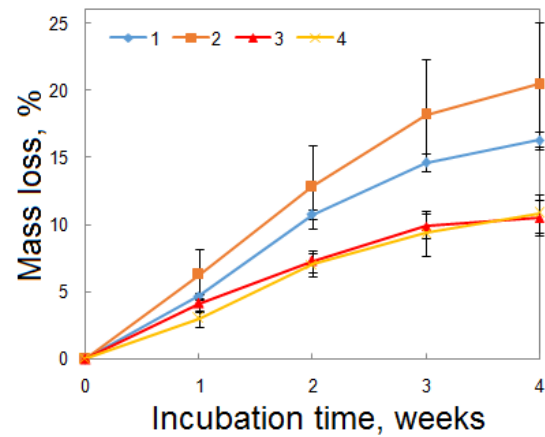


Figure 4 - Fatigue behaviour of the ZX10 (a) and WE43 (b) alloys in the initial states and after ECAP

It was shown that the grain refinement after ECAP leads to an increase in the fatigue limit of both studied alloys. In the case of the ZX10 alloy, the increase in fatigue limit is small, probably due to the formation of an unfavorable texture. So the fatigue limit of the alloy in the initial state was 100 MPa, and after ECAP - 110 MPa. For the WE43 alloy, the increase in the fatigue limit is more substantial: from 90 MPa in the initial state to 170 MPa after ECAP. One of the most important in-service properties of the magnesium medical alloys is their corrosion resistance. The corrosion resistance studies were carried out in a physiological saline solution of 0.9% NaCl at 37 °C in this work (Figure 2).



1 – ZX10 alloy in initial state; 2 – ZX10 alloy after ECAP; 3 – WE43 alloy in initial state; 4 – WE43 alloy after ECAP
Figure 5 – The study of corrosion resistance of the alloys

It was shown that the WE43 alloy has a higher corrosion resistance compared to the ZX10 alloy both in the initial state and after ECAP, apparently, due to the presence of rare-earth metals in the composition. Moreover, ECAP does not lead to a decrease in the corrosion resistance of both alloys. The total mass loss over 4 weeks of testing was 16.3 ± 0.6 and $20.4 \pm 4.7\%$ for the homogenized and deformed states of the ZX10 alloy and 10.5 ± 1.3 and $10.8 \pm 1.5\%$ for the homogenized and deformed states of the WE43 alloy, respectively.

4. Conclusions

1. ECAP leads to significant structure refinement of both studied alloys. For the WE43 alloy an UFG structure is formed with an average grain size of $0.69 \pm 0.13 \mu\text{m}$, as well as $\text{Mg}_{41}\text{Nd}_5$ phase particles with an average size of $0.45 \pm 0.18 \mu\text{m}$ during ECAP. ECAP processing of ZX10 alloy gave rise to grain refinement from $\sim 105 \mu\text{m}$ in the initial state to $4.0 \pm 0.19 \mu\text{m}$ and $8.0 \pm 0.18 \mu\text{m}$ in transversal and longitudinal cross-sections of the billets.
2. The grain refinement caused by ECAP of WE43 alloy result in improved strength characteristics ($Y_S = 260 \text{ MPa}$ and $UTS = 300 \text{ MPa}$), while also raising its tensile ductility to 12.4%. ECAP of ZX10 alloy was shown to moderately increase the mechanical strength of the alloy, while doubling its tensile elongation. The increasing of ductility is believed to be associated with the activation of prismatic slip.
3. A further positive effect of ECAP is an increase of the fatigue limit by $\sim 10\%$ on the ZX10 alloy and $\sim 89\%$ on the WE43 alloy.
4. The above beneficial effects were achieved without ECAP impairing the chemical corrosion resistance.

Acknowledgments

Funding support of this work was provided by the Russian Science Foundation (project #17-13-01488).

5. Literature

- [1] Y. Chen, Z. Xu, C. Smith et al. Recent advances on the development of magnesium alloys for biodegradable implants: Review // *Acta Biomater.*, 2014, 10, 4561-4573.
- [2] X. Li, X. Liu, S. Wu et al. Design of magnesium alloys with controllable degradation for biomedical implants: From bulk to surface // *Acta Biomater.*, 2016, 45, 2–30.
- [3] A. Atrens, M. Liu, N.I.Z. Abidin. Corrosion mechanism applicable to biodegradable magnesium implants // *Mater. Sci. Eng. B*, 2011, 176, 1609–1636.
- [4] Z. Li, X. Gu, S. Lou et al. The development of binary Mg–Ca alloys for use as biodegradable materials within bone // *Biomaterials*, 2008, 29(10), 1329–1344.
- [5] X.N. Gu, N. Li, Y.F. Zheng et al. In vitro degradation performance and biological response of a Mg–Zn–Zr alloy // *Mater. Sci. Eng. B*, 2011, 176(20), 1778–1784.

- [6] N.A. Agha, Z. Liu, F. Feyerabend et al. The effect of osteoblasts on the surface oxidation processes of biodegradable Mg and Mg-Ag alloys studied by synchrotron IR microspectroscopy // *Mater. Sci. Eng. C*, 2018, 91, 659–668
- [7] S. S. Nene, B. P. Kashyap, N. Prabhu et al. Biocorrosion and biodegradation behavior of ultralight Mg–4Li–1Ca (LC41) alloy in simulated body fluid for degradable implant applications // *J. Mater. Sci.*, 2015, 50(8), 3041–3050.
- [8] Y. Li, C. Wen, D. Mushahary et al. Mg–Zr–Sr alloys as biodegradable implant materials // *Acta Biomater.*, 2012, 8(8), 3177–3188.
- [9] L. Xu, G. Yu, E. Zhang et al. In vivo corrosion behavior of Mg–Mn–Zn alloy for bone implant application // *J. Biomed. Mater. Res.*, 2007, 83A(3), 703–711.
- [10] F. Witte, V. Kaese, H. Switzer et al. In vivo corrosion of four magnesium alloys and the associated bone response // *Biomaterials*, 2005, 26, 3557–3563.
- [11] R. Waksman, R. Pakala, P.K. Kuchulakanti et al. Safety and efficacy of bioabsorbable magnesium alloy stents in porcine coronary arteries // *Catheter. Cardiovasc. Interv.*, 2006, 68, 607–617.
- [12] I. Marco, A. Myrissa, E. Martinelli et al. In vivo and in vitro degradation comparison of pure Mg, Mg-10Gd and Mg-2Ag: a short term study // *Eur. Cell Mater.*, 2017, 33, 90–104.
- [13] R.Z. Valiev, A.P. Zhilyaev, T.G. Langdon. Bulk nanostructured materials: fundamentals and applications. Wiley, Hoboken, 2014.
- [14] R.Z. Valiev, R.K. Islamgaliev, I.V. Alexandrov. Bulk nanostructured materials from severe plastic deformation // *Prog. Mater. Sci.*, 2000, 45, 103–189.
- [15] P. Minárik, R. Král, M. Janeček. Effect of ECAP processing on corrosion resistance of AE21 and AE42 magnesium alloys // *Appl. Surf. Sci.*, 2013, 281, 44–48
- [16] E. Mostaed, M. Hashempour, A. Fabrizi et al. Microstructure, texture evolution, mechanical properties and corrosion behavior of ECAP processed ZK60 magnesium alloy for biodegradable applications // *J. Mech. Behav. Biomed.*, 2014, 37, 307–322
- [17] T.I. Savyolova, S.F. Kourtsov. ODF restoration by orientation grid // *Mater. Sci. Forum*, 2005, 459–457, 301–306.
- [18] V.N. Serebryany, L.L. Rokhlin, A.N. Monina. Texture and anisotropy of mechanical properties of the magnesium alloy of Mg-Y-Gd-Zr system // *Inorganic Materials: Applied Research*, 2014, 5(2), 116–123.
- [19] J. Groebner. Magnesium – Neodymium – Yttrium, in: G. Effenberg, F. Aldinger, P. Rogl (Eds.), *A comprehensive compendium of evaluated constitutional data and phase diagrams*, Volume 18, Stuttgart, 2001, 324–335.
- [20] S.R. Agnew, J.A. Horton, T.M. Lillo et al. Enhanced ductility in strongly textured magnesium produced by equal channel angular processing // *Scr. Mater.*, 2004, 50, 377–381.
- [21] P. Minárik, J. Veselý, R. Král et al. Exceptional mechanical properties of ultra-fine grain Mg-4Y-3RE alloy processed by ECAP // *Mater. Sci. Eng. A*, 2017, 708, 193–198.
- [22] J.-F. Nie. Precipitation and Hardening in Magnesium Alloys // *Metall. Mater. Trans.*, 2012, 43A(11), 3891–3939.